J Mater Sci (2007) 42:7702–7707
DOI 10.1007/s10853-007-1674-y

Experimental and numerical investigation on ductile-brittle fracture transition in a magnesium alloy

C. Yan · W. Ma · V. Burg · M. W. Chen

Received: 16 September 2005 / Accepted: 8 March 2007 / Published online: 3 June 2007

Abstract Tensile test on smooth and circumferentially notched specimens, systematic observation of fracture surfaces and large deformation finite element analysis were conducted to understand the deformation and failure behavior of a magnesium alloy (AM60). The plastic deformation is considered to be dominated by twining mediated slip. The tensile properties were not sensitive to the strain rates applied (3.3×10^{-4}~0.1). Corresponding to the same loading level, higher stress triaxiality but lower plastic strain was observed in the specimens with a smaller notch profile radius. Deformation and failure of the magnesium alloy were sensitive to the constraint level and ductile-brittle fracture transition occurred with decreasing the notch profile radius.

Introduction

Magnesium (Mg) alloys are attracting increasing attention due to potential applications in automobile, aerospace, communication and computer industry where light weight materials are desirable. Many investigations have been conducted to develop new Mg alloys with improved stiffness and ductility [1–3]. On the other hand, relatively less attention has been paid to the failure mechanisms of Mg alloys, such as brittle fracture, ductile tearing and ductile-brittle fracture transition, subjected to different environmental or loading conditions. As with metallic materials, failure is normally dependent on constraint (stress triaxiality) ahead of a crack or notch and brittle fracture is prompted by increasing crack length or sample thickness as a result of elevated constraint level. For structural steels, experimental observation and numerical analysis have demonstrated that fracture toughness estimated via crack tip opening displacement (CTOD) or *J*-integral at the initiation of a ductile crack is higher for specimens with low constraint than those with high constraint [4–7]. The phenomenon of ductile-brittle fracture transition has been observed in many engineering materials. For low and medium carbon structural steels, ductile-brittle transition is prompted by decreasing environmental temperature or increasing loading rate [8–9]. It was also demonstrated that ductile-brittle fracture transition in carbon steels was significantly affected by specimen geometry and crack length [10–11]. Therefore, failure mechanisms, especially the possibility of ductile-brittle transition in Mg alloys deserve further investigation. In this work, circumferentially notched tensile specimens were used to investigate the ductile-brittle fracture transition in an AM60 magnesium alloy under different constraint conditions. The effects of strain rate on yield stress and ductility were also studied. Large deformation finite element analysis was conducted to understand the stress–strain distributions in the notched specimens.

C. Yan (✉)
School of Engineering Systems, Queensland University of Technology, Brisbane, QLD 4001, Australia
e-mail: c2.yan@qut.edu.au

C. Yan · W. Ma
Centre for Advanced Materials Technology, School of Aerospace, Mechanical and Mechatronic Engineering, J07, The University of Sydney, Sydney, NSW 2006, Australia

V. Burg
Department of Mechanical Engineering, Eindhoven University of Technology, 5600 MB Eindhoven, The Netherlands

M. W. Chen
Institute for Materials Research, Tohoku University, Sendai 980-8577, Japan

Experimental and numerical analyses

Tensile test

AM60 cast magnesium alloy (with 6% Al, 0.2% Zn and 0.21%) was used in this work, which is one of the most popular magnesium alloys with great potential for applications in automotive industry. The microstructure is composed of α-Mg matrix and a second phase ($Mg_{17}Al_{12}$), as shown in Fig. 1. In order to vary the constraint condition, tensile test was carried out on circumferentially notched tensile bars with different notch profile radii (1, 2, 4 and 8 mm), whose dimensions are shown in Fig. 2. The specimens were machined from an ingot in the longitudinal direction. The tests were conducted using an Instron universal testing machine at a crosshead speed of 1 mm/min. The continuous change of the notch profile was monitored using a digital camera connected with a video recorder. Smooth tensile specimen (without notch) with a diameter of 5 mm was also tested under different strain rates (3.3×10^{-4}~10^{-1}). The axial strain was recorded using an extensometer mounted on the specimen surface. The fracture surfaces were examined using scanning electron microscopy (SEM).

Finite element analysis

To obtain a better understanding of the stress–strain distributions in the notched specimens, large deformation finite element analysis was carried out using MSC/MARC. Rate independent plasticity and associated flow rule were used for the material constitutive model. Isotropic hardening means that the yield function is written as

$$f(\sigma) = \bar{\sigma}(\varepsilon^{p}), \tag{1}$$

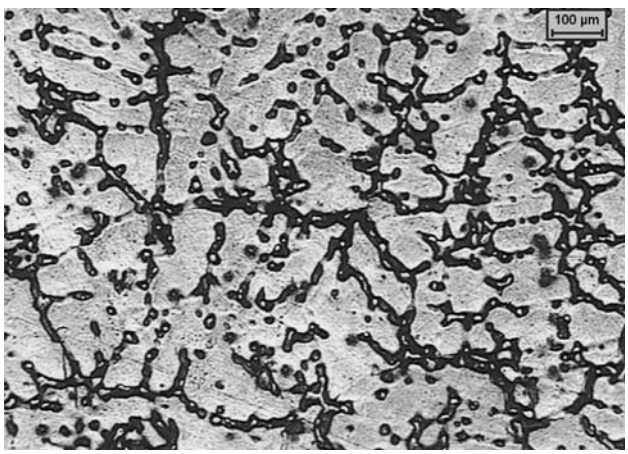

Fig. 1 Microstructure of the AM60 Mg alloy

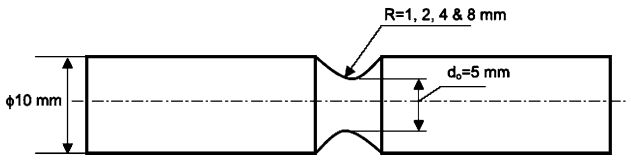

Fig. 2 Schematic of the circumferentially notched specimen

where ε^{p} is plastic strain and σ and $\bar{\sigma}$ are the Cauchy (true) stress and equivalent stress, respectively. The form of f employed in this study is the von Mises yield function

$$f(\sigma) = \left(\frac{3}{2}(\mathbf{s}_{ij}\mathbf{s}_{ij})\right)^{1/2}, \tag{2}$$

where $\mathbf{S}_{ij}$ is the deviatoric component of stress. The uniaxial true stress–strain curve estimated from the smooth tensile bars was input in the finite element program in a multi-linear form. Because the circumferentially notched specimen is axisymmetric, only a quarter of the specimen was modeled in 2-dimension to reduce the computational cost. The mesh size was optimized by carrying out mesh sensitive test with various element sizes. Small elements (about 10 μm) were placed in the notch root.

Results and discussion

Deformation in smooth tensile specimens

The typical stress–strain curve for the AM60 Mg alloy determined using the smooth tensile specimens is shown in Fig. 3, where apparent working hardening can be observed. It is interesting to note that some slip steps were developed

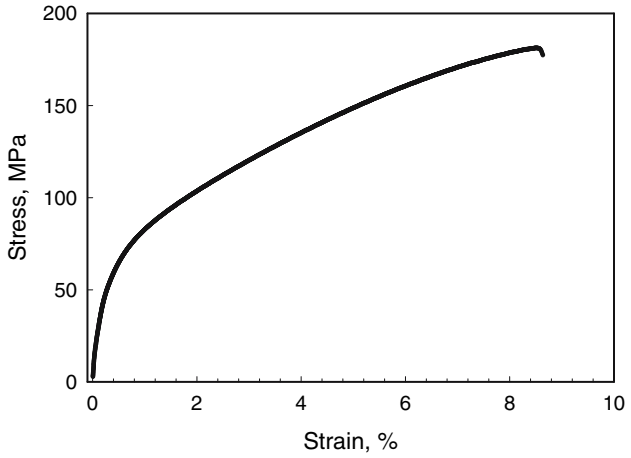

Fig. 3 Stress–strain behavior for the AM60 Mg alloy, determined using the smooth tensile specimens

on the specimen surface during the tensile test, as shown in Fig. 4a. To observe the microstructure close to the fracture surfaces, some broken tensile specimens were sectioned perpendicular to the fracture surfaces, polished and etched. The typical microstructure is illustrated in Fig. 4b. It can be seen that there are some deformation twins in the elongated microstructure. This is consistent with the observation of Gartnerova et al. [12] in an Mg alloy. Actually, it is not surprised to observe a deformation twin in a HCP metal like magnesium after some plastic deformation. As shown in Fig. 4a, extensive slip steps were developed, as a result of slip, i.e., motion of dislocations along the slip planes. Therefore, the effect of small amount of twining can be explained as the reorientations of the basal planes that then become more favorable relative to the stress axis such that the slip can take place. This has also been confirmed by Zhang et al [13]. The effect of strain rates on yield strength, tensile strength and elongation is shown in Table 1. In general, the tensile properties are not sensitive to the strain rates. The increase of yield strength with the strain rate is not significant and there is only a very slight decrease of the elongation at a high strain rate. For a HCP metal, higher ductility (elongation) can be obtained at higher strain rates due to increased working hardening rates. On the other hand, dynamic recovery may decrease the working hardening rates by lowering defect density [14]. These two effects may offset each other and lead to an almost constant ductility over the strain rates applied.

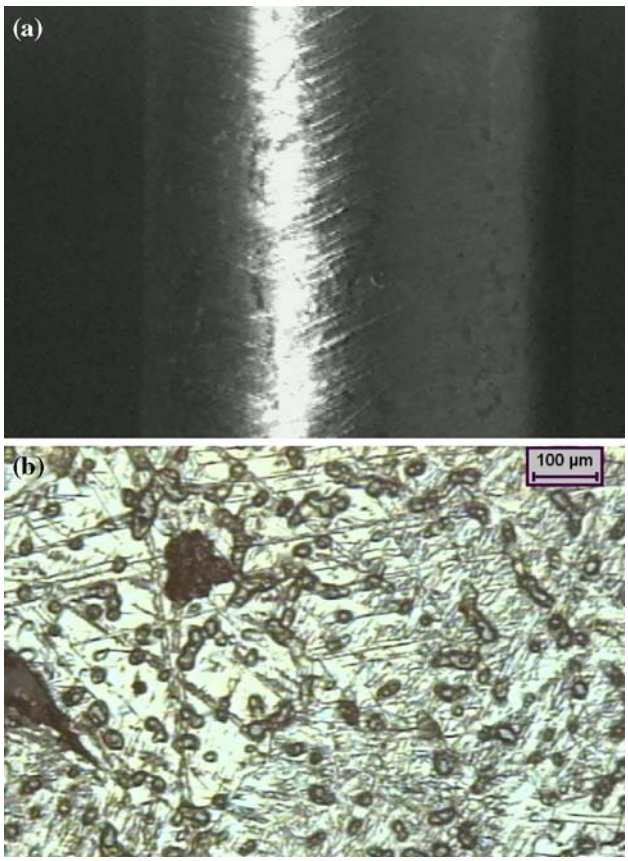

Fig. 4 (**a**) Slip lines on the tensile specimen surface, and (**b**) deformation twins observed in the microstructure close to the fracture surfaces

Table 1 Mechanical properties at different strain rates

Strain rate	Yield strength (MPa)	Ultimate tensile strength (MPa)	Elongation (%)
3.3×10^{-4}	56.6 ± 1.2	185.5 ± 3.2	8.5 ± 0.1
3.3×10^{-3}	55.4 ± 2.7	184.5 ± 2.4	8.4 ± 0.7
3.3×10^{-2}	63.4 ± 1.5	183.6 ± 3.2	8.2 ± 0.4
0.1	60.7 ± 1.1	180.4 ± 3.8	7.9 ± 0.1

Estimation of constraint in notched specimens

As mentioned before, deformation and failure of a metallic material may be very sensitive to constraint conditions. For a notched bar in tension, it is expected the deformation is not uniform in the axial direction within the notched section. The strain measured by the extensometer is only the average value within the total gauge length of the extensometer (50 mm). To clarify the variation of constraint with the notch radius in a quantitative way, the distributions of stresses and strains, especially the stress triaxiality (ratio between mean stress and effective stress) that is normally regarded as an indicator of constraint level, need to be estimated.

Figure 5 shows the finite element analysis of stress triaxiality and plastic strain along the diameter direction of the notched specimens at a load level of 4.5 kN. Apparently, the specimen with a smaller notch profile radius (R) has a higher level of stress triaxiality, i.e., a higher constraint level. It is interesting to note that the maximum stress triaxiality is located in the center of the notched specimens. On the other hand, a higher plastic strain is associated with the sample with a larger profile radius, i.e., lower constraint level, shown in Fig. 5b. Figure 6 shows the maximum stress triaxiality corresponding to the failure loads. It is clear that the maximum stress triaxiality decreases with increasing the notch profile radius. Figure 7 shows the effect of stress triaxiality on the tensile strength. It is clear that the tensile strength increases with the stress triaxiality. As compared to the smooth tensile specimen (Table 1), an apparent increase of tensile strength was observed in the notched specimens. Hancock and Mackenzie [15] have showed an apparent increase of fracture stress with stress triaxiality in two low alloy steels. Therefore, the notch profile radius has an apparent effect on the constraint level and tensile strength in this Mg alloy.

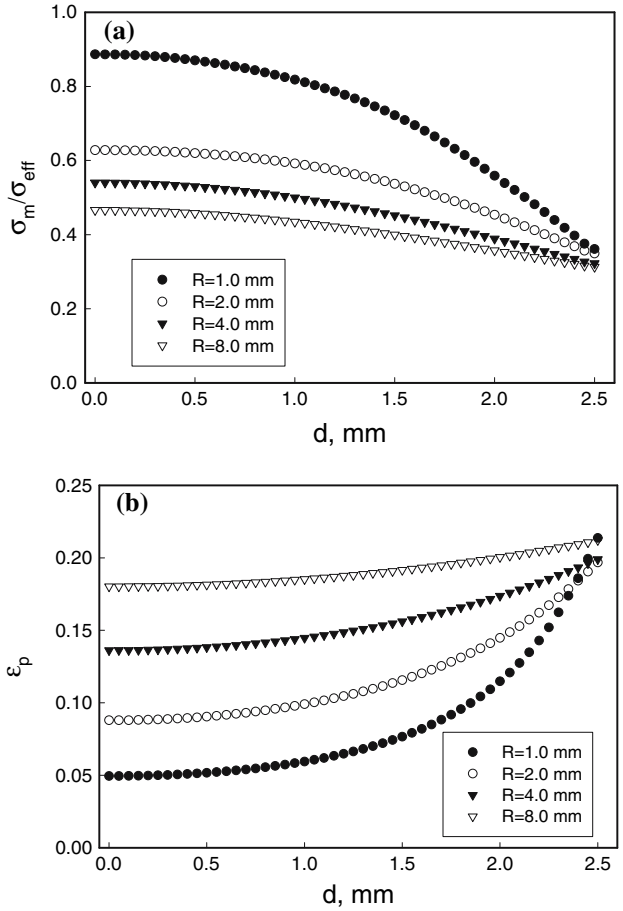

Fig. 5 Stress triaxiality (**a**) and plastic strain (**b**) along diameter direction of the notched specimens

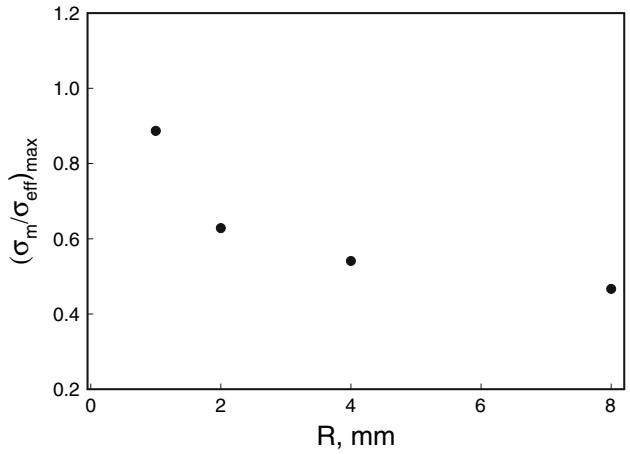

Fig. 6 Variation of the maximum stress triaxiality with notch radius

Ductile-brittle fracture transition

To gain a better understanding of the fracture mechanisms, the failure process of the notched bars was continuously monitored using a digital camera. The side views of the failed specimens are shown in Fig. 8. It can be seen in Fig. 8a that both the upper and lower fracture surfaces of the specimen (R = 1 mm) are perpendicular to the loading direction (specimen axis), indicating the predominant effect of normal stress on the final failure. Considering the high stress triaxiality in this specimen (Fig. 6), brittle fracture is expected. With increasing the notch profile radius, the fracture surfaces are gradually tilted to the loading direction, showing an increased influence of the shear stress, Fig. 8b–d. The corresponding fracture surfaces are shown in Fig. 9. For the samples with notch radius of 1 mm, the fracture surfaces are featured by cleavage facets, Fig. 9a. When the radius is increased from 2 mm to 8 mm, both amount and size of the dimples increase on the fracture surfaces. The fracture surfaces of the specimens with large notch profile radii (4 mm and 8 mm) are characterized by ductile fracture, Fig. 8c–d. Therefore, there is an apparent transition from ductile tearing to brittle fracture with decreasing the notch radius. As discussed by Ritchie et al. [16], the criterion of brittle fracture was postulated as the normal stress exceeding the cleavage stress over a characteristic distance. In this work, as shown in Fig. 6, there is an apparent increase of stress triaxiality when the notch profile radius is reduced. It is known that high stress triaxiality can greatly reduce the shear stresses that are regarded as the driving force for plastic deformation via slip or twining. As a result, plastic deformation is restricted as slip can only occur at a critical shear stress, i.e., resolved shear stress and brittle fracture is promoted when the normal stress reaches the cleavage stress. This is why brittle fracture was associated with the specimen with a small notch radius and there was a ductile-brittle transition when notch radius was reduced. Previous work on notched bend specimens also indicated an increase of normal stress ahead of a notch when the notch root radius was reduced, which prompted the occurrence of cleavage fracture [17].

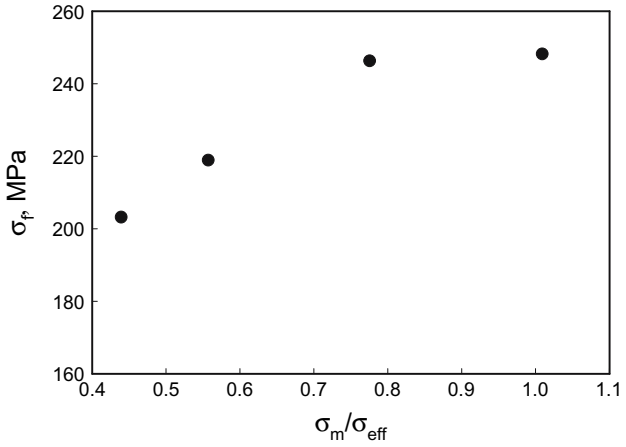

Fig. 7 Variation of tensile strength with stress triaxiality

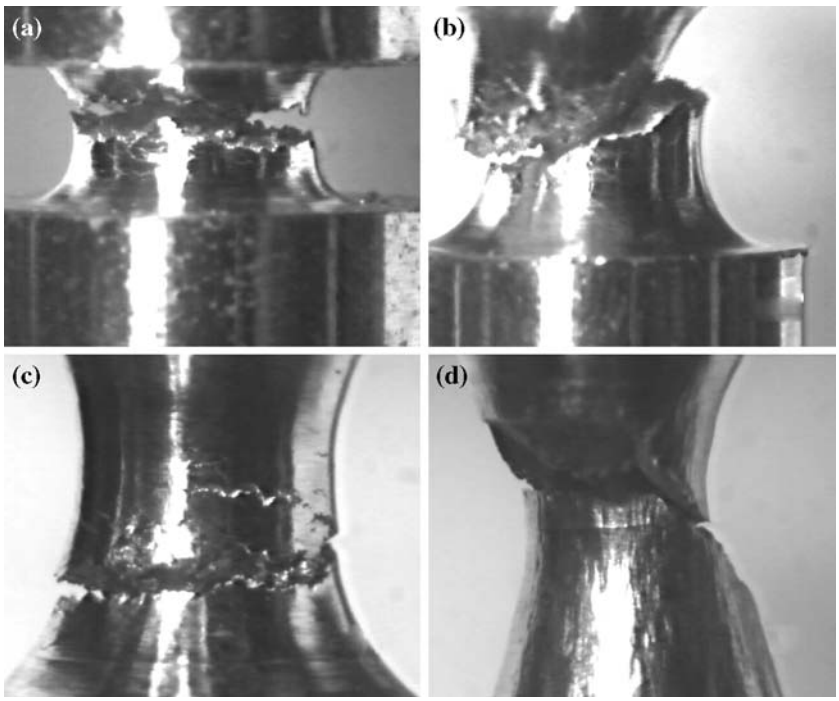

Fig. 8 Side views of the notched specimen after failure: (**a**) R = 1 mm, (**b**) R = 2 mm, (**c**) R = 4 mm and (**d**) R = 8 mm

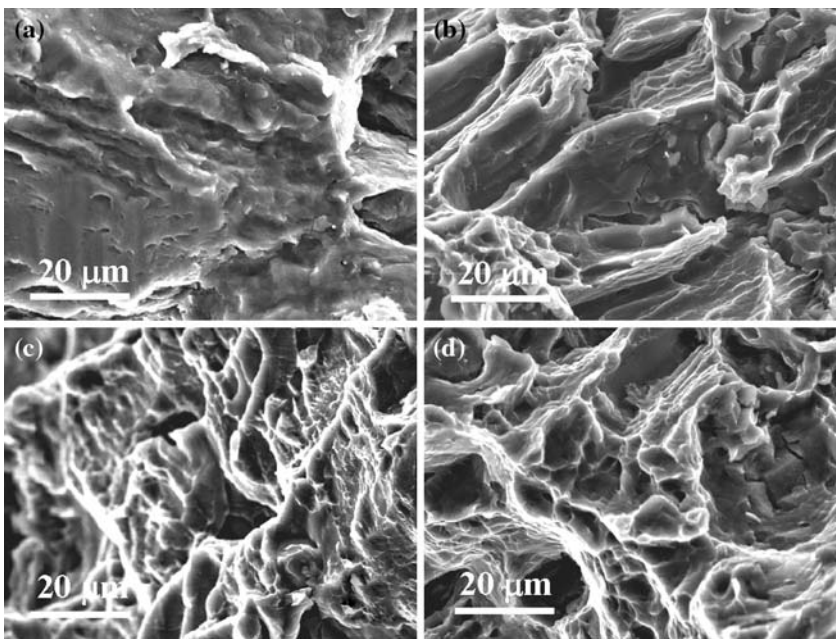

Fig. 9 Typical fracture surfaces of the notched specimens: (**a**) R = 1 mm, (**b**) R = 2 mm, (**c**) R = 4 mm and (**d**) R = 8 mm

Therefore, the failure mechanisms of the magnesium alloy are sensitive to the constraint level and apparent embrittlement is expected under high constraint conditions.

Conclusions

Smooth and circumferentially notched tensile specimens were used to investigate the deformation and failure behavior of an AM60 Mg alloy. Large deformation finite element analysis was also conducted to estimate the stress triaxiality (constraint) in the notched specimens. The tensile test using the smooth bars indicated that the mechanical properties were not sensitive to the strain rates applied (3.3×10^{-4}~0.1) and the plastic deformation was dominated by twining mediated slip. Corresponding to the same loading level, higher stress triaxiality but lower plastic strain was observed in the specimens with a smaller notch

profile radius. Higher tensile strength was associated with the specimens with higher stress triaxiality. The ductile-brittle fracture transition occurred when the notch profile radius was reduced from 8 mm to 1 mm due to the increase of constraint. Therefore, apparent embrittlement is expected for this alloy under high constraint conditions.

Acknowledgements C. Yan wishes to acknowledge the support of an ARC Discovery Project and a Sydney University Sesqui R & D grant.

References

1. Lu L, Raviprasad K, Lai MO (2004) Mater Sci Eng A368:117
2. Singh A, Watanabe M, Kato A, Tsai AP (2004) Scripta Mater 51:955
3. Kim HK, Lee YI, Chung CS (2005) Scripta Mater 52:473
4. Cotterell B, Li QF, Zhang DZ, Mai Y-W (1985) Eng Fract Mech 21:239
5. Matsoukas G, Cotterell B, Mai Y-W (1986) Eng Fract Mech 23:661
6. Wu SX, Mai Y-W, Cotterell B, Lee CV (1991) Acta Metall Mater 39:2527
7. Yan C, Mai Y-W (1998) Int J Fract 92:287
8. Knott JF (1973) Fundamentals of fracture mechanics. Butterworths, London
9. Atkins AG, Mai Y-W (1985) Elastic and plastic fracture. John Wiley/Ellis Horwood, Chichester
10. Yan C, Y-W Mai (2000) Int J Press Vessels Piping 77:313
11. Yan C, Mai Y-W, Wu SX (1997) Int J Fract 87:345
12. Gartnerova V, Trojanova Z, Jager A, Palcek P (2004) J Alloys Compd 378:180
13. Zhang P, Watzinger B, Kong PQ, Blum W (2000) Key Eng Mater 17–174:609
14. Han BQ, Huang JY, Zhu YT, Lavernia EJ (2006) Scripta Mater 54:1175
15. Hancock JW, Mackenzie AC (1976) J Mech Phys Solids 24:147
16. Ritchie RO, Knott JF, Rice JR (1973) J Mech Phys Solids 21:395
17. Yan C, Chen JH, Sun J, Wang Z (1993) Metall Trans 24A:1381